Acta Mech 233, 3213–3231 (2022)
https://doi.org/10.1007/s00707-022-03280-w

ORIGINAL PAPER

Yiyuan Jiang · Li Li · Yujin Hu

Strain gradient elasticity theory of polymer networks

Received: 3 March 2022 / Revised: 8 May 2022 / Accepted: 12 June 2022 / Published online: 9 July 2022

Abstract In physically (statistically) based theories for rubber-like materials, network models serve as a bridge that connects chain dynamics to continuum constitutive relations. However, there is no existing network model that accounts for the size-dependent mechanical properties of nano/microsize polymeric structures. The present work aims to fill this gap and derive a physically based strain gradient continuum. To establish a quantitative relation between the microscopic Helmholtz free energy due to polymer chain stretch and the macroscopic counterpart that depends on all details of the strain field, we connect strain and strain gradient measures to the positions of all chain ends. Taking the continuum displacement field to be interpolatory at the chain ends, a general framework is constructed, which is not restricted to any specific network structure. Applying the general framework to the commonly used 8-chain network model, we derive a first-order strain gradient elastic continuum, where size of the representative network turns out to be the characteristic length scale of strain gradient material. According to the scalar invariants of strain gradient tensor that remain at last, the assumption of parameter reduction in the simplified strain gradient elasticity theory is justified.

1 Introduction

The wide application of polymers in engineering requires the effectiveness of design and simulation, which puts forward a demand for an appropriate constitutive model [1] that enables to capture its complicated behavior, including nonlinear elasticity, visco-elastic-plastic phenomena and the so-called Mullins effect, etc. As a polymeric structure can be made small and smaller, with the development of manufacturing techniques, variations of its mechanical properties with the overall size should also be taken into account [2,3].

Physically based constitutive theories of rubber take a bottom-up approach. The energetics of every single chain can be analyzed through statistical mechanics, and then through synthesizing the accurate results obtained at the bottom level, it is hopeful to derive the description of macroscopic polymeric structures [4–8]. However, a critical component is missing in the bottom-up procedure: we have no idea how the conformation of a chain is geometrically related to the configuration of macroscopic continuum. The relation must be assumed manually, and therefore several network models appear in order to provide this connection, such as the 3-chain model [9], 4-chain model [10,11], 8-chain model [12], and the non-affine microsphere model [13–15]. For a detailed comparison of rubber-network models, reader can refer to [1,8]. Each network model aims to improve upon previous ones in either the number of parameters to calibrate, or the stretch range of validity.

Y. Jiang · L. Li (✉)· Y. Hu (✉)
State Key Laboratory of Digital Manufacturing Equipment and Technology, School of Mechanical Science and Engineering, Huazhong University of Science and Technology, Wuhan 430074, China
E-mail: lili_em@hust.edu.cn

Y. Hu
E-mail: yjhu@hust.edu.cn

However, to the best knowledge of authors, there is no existing network model accounting for the size dependence of mechanical properties of nano/microsize polymeric structures. With the development of manufacturing techniques [2], the polymeric structure can be made small enough to exhibit size effects, which is substantiated by experiments [3], where the normalized bending rigidity of the polymeric beams are found to be size-dependent. We aim to construct a network model that connects conformation of chains to the configuration of continuum with size-dependent properties.

To capture size effects, several generalized continuum theories have been proposed, among which commonly used are the strain gradient elasticity [16–18], integral-type nonlocal elasticity [19,20], and micromorphic theory [21,22]. All the information about size dependence of properties are encoded in the intrinsic length and additional parameters [23,24]. Although the abovementioned theories show great success in predicting mechanical behaviors of micro/nanostructures [25–30], however, they suffer from two apparent and widely acknowledged shortcomings. One is the ambiguous and controversial physical interpretations of the intrinsic length. [31–35], and the other is too many parameters to calibrate [36,37]. For example, in Mindlin's strain gradient elasticity theory [16], we need five additional parameters to determine the energy of an isotropic material, which is difficult to implement. To improve the latter shortcoming, a simplified strain gradient elasticity theory (SSGET) [38,39] is later developed with reduction of parameters. This reduction, however, is not rigorously justified in the original work. Recently, there have been many efforts contributing to homogenizing heterogeneous materials to strain gradient media, where the intrinsic length, the additional constants and the assumption for parameter reduction may hopefully be physically interpreted [40–43].

The chain conformation is governed by its energetics and the strain gradient continuum is governed by its constitutive relations. If a rigorous connection can be established between the chain conformations and the strain gradient continuum configurations, a quantitative relation can be established between two expressions of energy: the microscopic expression for free energy due to chain stretch and the macroscopic counterpart that depends on all details of the strain field. In this way the size-dependent properties of nano/microsize polymeric structures can be captured by the derived strain gradient continuum, where the artificially introduced characteristic length shall be equipped with a clear physical interpretation by the concrete geometry of network. Furthermore, if only a few scalar invariants of strain gradient tensor remain at last, the assumption of parameter reduction in the simplified strain gradient elasticity theory (SSGET) can be justified.

In this work, we aim to establish the connection between chain conformations and strain gradient configurations. First, a general framework is proposed, which puts no restriction on geometry of network structure. The order of strain gradient continuum depends on the specific network geometry. Next, a first-order strain gradient constitutive relation is derived by applying the general framework to the "8-chain" network.

2 Problem statement

In this study, we seek to derive a physically based strain gradient continuum which can only be possible when a connection between the conformation of a chain and the configuration of a strain gradient continuum is established. The conformation of a chain is governed by the chain dynamics, which is described accurately by statistical mechanics.

2.1 Energetics of a single polymer chain

In theory of statistical mechanics, taking one end of the polymer chain as the origin, each point in space is equipped with a probability density describing how likely for the other end to reside in the neighborhood (Fig. 1). For instance, the Gaussian statistics assumes an isotropic probability density distribution $P(\boldsymbol{r})$, i.e., $P(\boldsymbol{r}) = P(|\boldsymbol{r}|)$ does not depend on the direction angles (β, θ).

When a single chain stretches, its end moves to another point with less probability density, resulting in the decrease of entropy, and thus the increase of Helmholtz free energy. Ultimately, resistance to energy increase gives resistance to tension. For freely jointed chains [5], Gaussian statistics and the Langevin statistics render two common approaches, and the latter extends the former via accounting for limited extendability. The explicit expression of free energy will be provided in a later section (Eq. (2)) and immediately used.

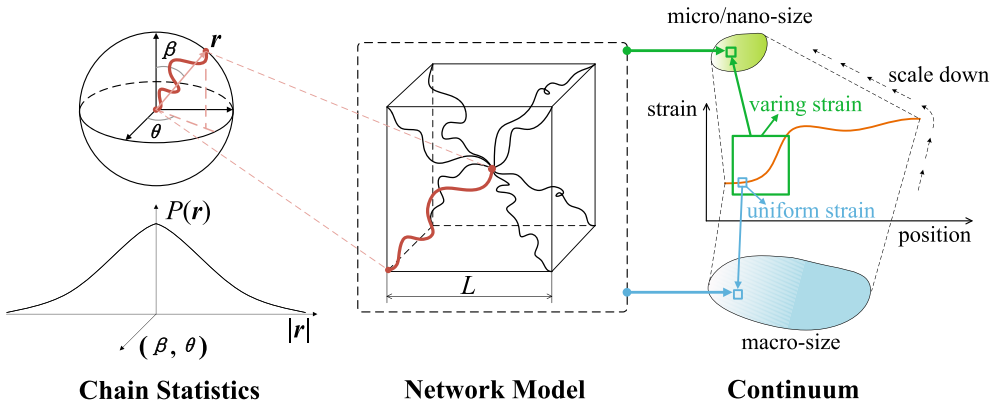

Fig. 1 The chain-network-continuum bottom-up procedure

2.2 Importance of strain gradients

Effective moduli of micropolymeric beams have been found size-dependent by bending experiments where large gradients of strain field exist [3]. To see why a large strain gradient makes a difference for microstructures, we need to take a closer look at the network models. For instance, as shown in Fig. 1, in the existing 8-chain network model, eight equivalent chains start from eight vertices of a cube and join at the center. Size of the cube (side length L) is negligible compared to macro-structures, which renders the cube as an infinitesimal differential element of the macro-size continuum, where the strain field inside is viewed uniform. However, for micro/nanosize continuum, the cube cannot be taken as infinitesimal, and thus it may perceive finite variations of strain field (Fig. 1).

The strain field can be approximated by its Taylor expansion in spatial variables, where the coefficients render the source of high-order strain measure (see Eq. (3)), i.e., strain gradients (of arbitrary order). When the strain gradients are large, their effects cannot be neglected. Qualitatively speaking, when the average strain is the same, i,e., fixing eight vertices of the cube, changes in the position of the connection point will result in different values of total Helmholtz energy of the eight chains. In other words, in order to derive the strain gradient continuum, eight chains inside the network are allowed to undergo different stretch.

2.3 The key problem in connecting chain conformations and strain gradient continuum configurations

The chain conformation is governed by its energetics and the strain gradient continuum is governed by its constitutive relations. In deriving the physically based (bottom up) strain gradient theory of rubber, the only thing missing is the connection between chain conformation and the strain gradient continuum configuration, which is completely geometric.

On one hand, in the statistical description of a single chain, all that matters is the relative position of chain ends. For example, in the eight-chain network, all the microscopic information is encoded in 9 (8 vertices and 1 connection points) discrete points. On the other hand, in continuum description, the total strain energy depends on all details of the entire strain field inside.

We aim to construct the abovementioned connection, which poses the key problem: to derive the strain and strain gradients measure from positions of all the chain ends.

3 General framework

In this section, we connect chain conformations and strain gradient continuum configurations. A general framework is proposed, which puts no restrictions on geometry of networks. In this work, we focus on size-effects and assume infinitesimal strain with large strain gradients.

3.1 Two versions of free energy

In order to proceed, we need to check what is available. We have two expressions for the same free energy. The microscopic expression is obtained through statistical mechanics and provides physical interpretations for the macroscopic counterpart.

3.1.1 Helmholtz free energy in terms of statistical mechanics

Considering the freely jointed chains which permit the additivity of energy [5], the total Helmholtz free energy W_{micro} inside the representative volume is given as the sum of contributions from all chains inside (total number of chains denoted by N_C), i.e.,

$$W_{\text{micro}} = \sum_{N=1}^{N_C} W_N. \tag{1}$$

For mild stretch, the Gaussian statistics renders an accurate description [5], which gives the Helmholtz free energy of a single chain as

$$W_N = \frac{3}{2} k_{\text{B}} T \left(\frac{r_N}{r_0} \right)^2 = \frac{3}{2} k_{\text{B}} T \lambda_N^2, \tag{2}$$

where k_{B} is the Boltzmann constant and T is the absolute temperature. The Nth chain stretches from its initial end-to-end distance r_0 (where we assume that all chains equal the initial length) to the final value r_N, having the stretching ratio:

$$\lambda_N = \frac{r_N}{r_0}.$$

It can be observed from Eq. (2) that the free energy is proportional to temperature. The higher the temperature is, the larger the free energy becomes.

In this study, we only consider the isothermal condition. Thus, the free energy is only proportional to the stretching ratio λ_N. Furthermore, we assume that $\lambda_N \to 1$.

3.1.2 Helmholtz free energy in the viewpoint of continuum mechanics

The representative volume V_{rt} is viewed as a rather small (but not infinitesimal) part of the continuum, inside which the displacement field can be approximated by its Taylor expansion in space variables $\boldsymbol{x}$ as follows [31,34]:

$$\boldsymbol{u}(\boldsymbol{x}) = \boldsymbol{u}_0 + \boldsymbol{A}_1 \cdot \boldsymbol{x} + \frac{1}{2!} \boldsymbol{A}_2 : (\boldsymbol{x} \otimes \boldsymbol{x}) + \frac{1}{3!} \boldsymbol{A}_3 \vdots (\boldsymbol{x} \otimes \boldsymbol{x} \otimes \boldsymbol{x}) + \ldots \quad (\boldsymbol{x} \in V_{rt}), \tag{3}$$

where "$\cdot$," "$:$," "$\vdots$" denote scalar products of vectors, second-order tensors and third-order tensors, respectively; and $\boldsymbol{A}_1$, $\boldsymbol{A}_2$, $\boldsymbol{A}_3$ are *constant* second-order, third-order and fourth-order tensors, respectively; $\boldsymbol{u}_0$ denotes the original displacement at the center of a representative volume; and $\otimes$ is the tensor product. These tensors render the source of higher-order strain measure, and the order of strain gradient continuum depends on the order of truncation. Distribution of displacement field inside the representative volume V_{rt} determines the total Helmholtz free energy inside, i.e.,

$$W_{\text{macro}} = W_{\text{macro}}[\boldsymbol{u}], \tag{4}$$

where the square bracket denotes W_{macro} as a functional of $\boldsymbol{u}$.

Deriving a physically based strain gradient continuum constitutive relation means to find a quantitative relation between the two energies, which will only be possible when we establish the connection between chain conformations and strain gradient continuum configurations.

3.2 Connection between chain conformations and strain gradient continuum configurations

Based on the following considerations:

(a) Microscopically, the free energy of a freely jointed chain only depends on the stretching ratio, which can be completely determined by specifying the position of its two ends. Therefore, the total free energy is given as

$$W_{\text{micro}} = W_{\text{micro}}\left(\boldsymbol{r}_1^{(1)}, \boldsymbol{r}_2^{(1)}, ..., \boldsymbol{r}_1^{(N_c)}, \boldsymbol{r}_2^{(N_c)}\right), \tag{5}$$

where $\boldsymbol{r}_1^{(i)}, \boldsymbol{r}_2^{(i)}$ denote the position vectors at two ends of the ith chain (Fig. 2). In other words, the *microscopic* information is concentrated in a few discrete points (chain ends).

(b) Macroscopically, once we adopt the polynomial form (3), the functional dependence of free energy W_{macro} on the whole displacement field reduces to function dependence on the constant coefficients $(\boldsymbol{A}_1)_{ij}$, $(\boldsymbol{A}_2)_{ijk}$, $(\boldsymbol{A}_3)_{ijkl}$, etc if we process a volume integration. That is,

$$W_{\text{macro}}[\boldsymbol{u}] = W_{\text{macro}}(\boldsymbol{A}_1, \boldsymbol{A}_2, \boldsymbol{A}_3, ...), \tag{6}$$

where square brackets denote functional dependence, and round brackets denote function dependence. In other words, the macroscopic kinematic information is concentrated in finitely many variables.

We establish the connection (Fig. 2).

The chains lie in the representative volume with the displacement field (3) *specified for each point in space, and the displacement field is taken to be interpolatory at the chain ends.* Mathematically,

$$\begin{aligned}
\boldsymbol{r}_1^{(1)} - \boldsymbol{r}_{01}^{(1)} &=: \boldsymbol{u}_1^{(1)} = \boldsymbol{u}\left(\boldsymbol{r}_{01}^{(1)}\right) \\
\boldsymbol{r}_2^{(1)} - \boldsymbol{r}_{02}^{(1)} &=: \boldsymbol{u}_2^{(1)} = \boldsymbol{u}\left(\boldsymbol{r}_{02}^{(1)}\right) \\
&... \\
\boldsymbol{r}_1^{(N_C)} - \boldsymbol{r}_{01}^{(N_C)} &=: \boldsymbol{u}_1^{(N_C)} = \boldsymbol{u}\left(\boldsymbol{r}_{01}^{(N_C)}\right) \\
\underbrace{\boldsymbol{r}_2^{(N_C)} - \boldsymbol{r}_{02}^{(N_C)} =: \boldsymbol{u}_2^{(N_C)}}_{\text{microscopic}} &= \underbrace{\boldsymbol{u}\left(\boldsymbol{r}_{02}^{(N_C)}\right)}_{\text{macroscopic}}
\end{aligned} \tag{7}$$

where we have two sets of descriptions:

(a) Microscopic descriptions include $\boldsymbol{r}_{01}^{(1)}, \boldsymbol{r}_{02}^{(1)}, ..., \boldsymbol{r}_{01}^{(N_c)}, \boldsymbol{r}_{02}^{(N_c)}$ that denote initial positions of chain ends, $\boldsymbol{r}_1^{(1)}, \boldsymbol{r}_2^{(1)}, ..., \boldsymbol{r}_1^{(N_c)}, \boldsymbol{r}_2^{(N_c)}$ that denote final positions, and $\boldsymbol{u}_1^{(1)}, \boldsymbol{u}_2^{(1)}, ..., \boldsymbol{u}_1^{(N_C)}, \boldsymbol{u}_2^{(N_C)}$ that denote the thus defined displacement vectors.

(b) Macroscopic descriptions include $\boldsymbol{u}\left(\boldsymbol{r}_{01}^{(1)}\right), \boldsymbol{u}\left(\boldsymbol{r}_{02}^{(1)}\right), ..., \boldsymbol{u}\left(\boldsymbol{r}_{01}^{(N_C)}\right), \boldsymbol{u}\left(\boldsymbol{r}_{02}^{(N_C)}\right)$ that denote the values of continuum displacement field taken at corresponding points.

Equations (3) and (7) give $\boldsymbol{r}_1^{(1)}, \boldsymbol{r}_2^{(1)}, ..., \boldsymbol{r}_1^{(N_c)}, \boldsymbol{r}_2^{(N_c)}$ as functions of $\boldsymbol{A}_1, \boldsymbol{A}_2, \boldsymbol{A}_3, ...$, and thus we may tie W_{micro} to W_{macro} in the following way

$$W_{\text{macro}}(\boldsymbol{A}_1, \boldsymbol{A}_2, \boldsymbol{A}_3, ...) = \Delta W_{\text{micro}}\left(\boldsymbol{r}_1^{(1)}(\boldsymbol{A}_1, \boldsymbol{A}_2, \boldsymbol{A}_3, ...), \boldsymbol{r}_2^{(1)}(\boldsymbol{A}_1, \boldsymbol{A}_2, \boldsymbol{A}_3, ...), ...\right), \tag{8}$$

where the zero of W_{macro} corresponds to initial values of W_{micro}, i.e.,

$$\Delta W_{\text{micro}} := W_{\text{micro}}\left(\boldsymbol{r}_1^{(1)}, \boldsymbol{r}_2^{(1)}, ..., \boldsymbol{r}_1^{(N_c)}, \boldsymbol{r}_2^{(N_c)}\right) - W_{\text{micro}}\left(\boldsymbol{r}_{01}^{(1)}, \boldsymbol{r}_{02}^{(1)}, ..., \boldsymbol{r}_{01}^{(N_c)}, \boldsymbol{r}_{02}^{(N_c)}\right). \tag{9}$$

As a scalar quantity, W_{macro} is invariant with respect to coordinate transformation and thus should be able to be expressed by scalar invariants [44]. Then, Eq. (8) can be ultimately given as

$$W_{\text{macro}}(\text{Invarants}\{\boldsymbol{A}_1, \boldsymbol{A}_2, \boldsymbol{A}_3, ...\}) = \Delta W_{\text{micro}}\left(\boldsymbol{r}_1^{(1)}, \boldsymbol{r}_2^{(1)}, ..., \boldsymbol{r}_1^{(N_c)}, \boldsymbol{r}_2^{(N_c)}\right), \tag{10}$$

where "Invarants$\{\boldsymbol{A}_1, \boldsymbol{A}_2, \boldsymbol{A}_3, ...\}$" denote the invariants of all possible combinations of $\boldsymbol{A}_1, \boldsymbol{A}_2, \boldsymbol{A}_3, ...$

In this section, we make no restrictions on any geometrical details of the representative network, In the next section, we follow the general framework proposed in this section to form a concrete constitutive model.

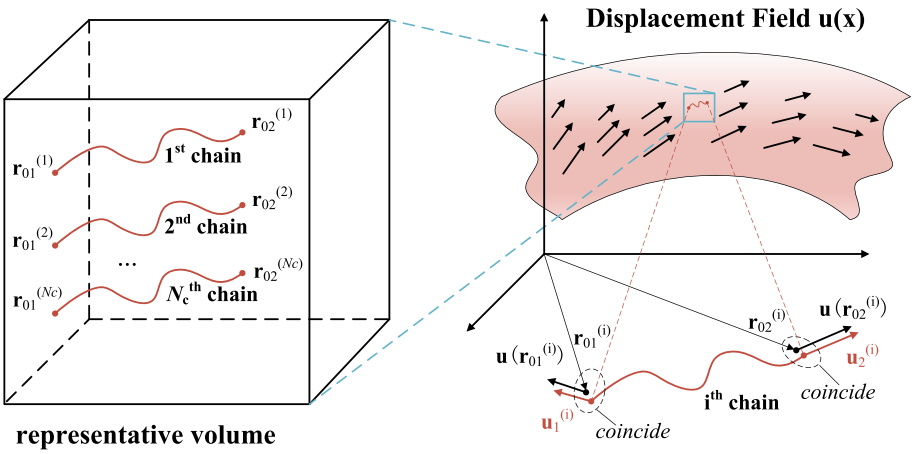

Fig. 2 The connection between chain conformations and continuum configurations

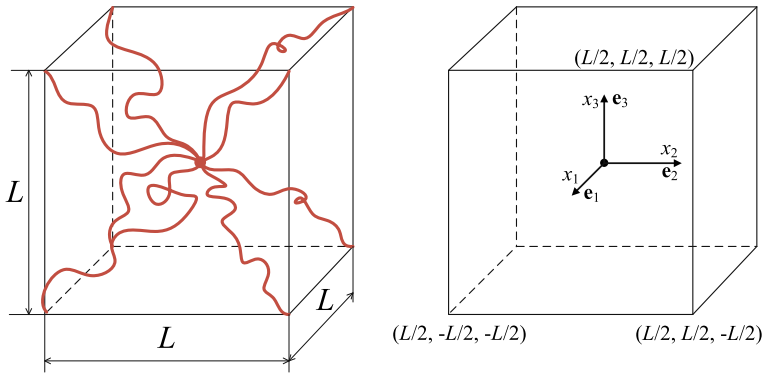

Fig. 3 Illustration of the 8-chain network

4 Strain gradient elasticity based on the eight-chain model

In this section, we proceed with the general framework further by applying it to a concrete network structure. The "8-chain" network is adopted (Fig. 3). The representative volume is a cube with length L, occupying the three-dimensional space $\left[-\frac{L}{2}, \frac{L}{2}\right] \times \left[-\frac{L}{2}, \frac{L}{2}\right] \times \left[-\frac{L}{2}, \frac{L}{2}\right]$. The Cartesian coordinate system is shown in Fig. 3, the origin being at the center of the cube.

4.1 Microscopic and macroscopic descriptions of the eight-chain network

As for the total Helmholtz free energy W_{micro} inside the representative volume, we have the number of chains $N_C = 8$ and Eq. (1) becomes

$$W_{\text{micro}} = \sum_{N=1}^{8} W_N, \tag{11}$$

where W_N is given by Eq. (2):[1]

$$W_N = \frac{3}{2} k_{\text{B}} T \left(\frac{r_N}{r_0}\right)^2 = \frac{3}{2} k_{\text{B}} T \lambda_N^2.$$

[1] Note that in the original work proposing the "8-chain" network [12], Langevin statistics is used to account for limited extendability. However, in the present work, we focus on large strain gradients instead of large finite strain, and thus the Gaussian statistics renders accurate.

As for the macroscopic expression of Helmholtz free energy W_{macro}, the first step is to assign the displacement field. Since the free energy is invariant with respect to rigid-body motions, we impose an additional translation such that the displacement at the origin is zero, i.e., $\boldsymbol{u}_0 = 0$ in Eq. (3). Therefore, eight chain-ends at the eight vertices of the cube render the complete microscopic description, resulting in 24 independent variables which account for 3 displacement components of the 8 vertices. In the macroscopic counterpart, we may have the same number of independent variables by truncating the Taylor expansion (3): (Here we use another set of notations for the coefficients $\boldsymbol{A}_1 \to \boldsymbol{E}$, $\boldsymbol{A}_2 \to \boldsymbol{D}$, the convenience of which will be illustrated by their physical meanings later in this section)

$$\boldsymbol{u}(\boldsymbol{x}) = \boldsymbol{E} \cdot \boldsymbol{x} + \frac{1}{2}\boldsymbol{D} : (\boldsymbol{x} \otimes \boldsymbol{x}), \tag{12}$$

where the second-order tensor $\boldsymbol{E}$ and the third-order tensor $\boldsymbol{D}$ are constant, equipped with the following symmetry

$$E_{ij} = E_{ji}, D_{ijk} = D_{ikj}. \tag{13}$$

Indices i (j, k) take values of 1, 2, 3, and summation is invoked on repeated indices (in the following). We arrived at total $(6 + 18 = 24)$ coefficients. The corresponding strain and strain gradient render

$$\begin{aligned} \langle \boldsymbol{\varepsilon} \rangle &= \left\langle \frac{1}{2}(\boldsymbol{u}\nabla + \nabla \boldsymbol{u}) \right\rangle = \boldsymbol{E}, \\ \langle \boldsymbol{\varepsilon}\nabla \rangle &= \boldsymbol{\varepsilon}\nabla = \frac{1}{2}\left(D_{ijk} + D_{jik}\right) \boldsymbol{e}_i \otimes \boldsymbol{e}_j \otimes \boldsymbol{e}_k, \end{aligned} \tag{14}$$

where "$\langle \cdot \rangle$" denotes volume average, "∇" denotes the nabla operator, and $\boldsymbol{e}_i$ $(i = 1, 2, 3)$ denotes the Cartesian basis vector (Fig. 3).

4.2 Non-dimensionalization

To proceed further, we rearrange all equations in a dimensionless setting. A new coordinate ξ_j is adopted such that

$$-\frac{1}{2} \le \xi_j = \frac{x_j}{L} \le \frac{1}{2}. \tag{15}$$

The dimensionless displacement field can then be expressed as

$$\frac{u_i}{L} = E_{ij}\xi_j + \frac{1}{2}L D_{ijk}\xi_j\xi_k. \tag{16}$$

Since the volume-averaged strain gradient tensor only depends on the combination $\frac{1}{2}\left(D_{ijk} + D_{jik}\right)$, we may equip the third-order tensor $\boldsymbol{D}$ with additional symmetry:

$$D_{ijk} = D_{jik} \tag{17}$$

which qualifies it as the strain gradient tensor. Introducing the notations $\bar{u}_i = \frac{u_i}{L}$, $H_{ijk} = L D_{ijk}$, Eq. (16) becomes

$$\bar{u}_i = E_{ij}\xi_j + \frac{1}{2}H_{ijk}\xi_j\xi_k. \tag{18}$$

The dimensionless Helmholtz free energy of a single chain is defined as

$$\bar{W}_N := \frac{W_N}{\frac{3}{2}k_{\text{B}}T} = \lambda_N^2 \tag{19}$$

which is given in terms of displacement as

$$\begin{aligned}\bar{W}_N &= \lambda_N^2 \\ &= \left(\frac{r_N}{r_0}\right)^2 \\ &= \frac{r_N^2}{\frac{3}{4}L^2} \\ &= \frac{\boldsymbol{u}^2(\boldsymbol{x}_N) + \boldsymbol{x}_N^2 + 2\boldsymbol{u}(\boldsymbol{x}_N)\cdot\boldsymbol{x}_N}{\frac{3}{4}L^2} \\ &= \frac{4}{3}\bar{\boldsymbol{u}}^2(\boldsymbol{\xi}_N) + 1 + \frac{8}{3}\bar{\boldsymbol{u}}(\boldsymbol{\xi}_N)\cdot\boldsymbol{\xi}_N,\end{aligned} \tag{20}$$

where the square of the initial chain length is $r_0^2 = \frac{3}{4}L^2$ in the "eight-chain" representative volume. The link (Eq. (7)) between microscopic and macroscopic descriptions of deformation is invoked, where $\boldsymbol{x}_N$ is the position vector of the Nth chain end on the vertex, non-dimensionalized as $\boldsymbol{\xi}_N$ according to Eq. (15). The change in free energy ΔW_N is given by subtracting the initial free energy from Eq. (20):

$$\Delta\bar{W}_N(\boldsymbol{\xi}_N) = \frac{4}{3}\bar{\boldsymbol{u}}^2(\boldsymbol{\xi}_N) + \frac{8}{3}\bar{\boldsymbol{u}}(\boldsymbol{\xi}_N)\cdot\boldsymbol{\xi}_N \tag{21}$$

which only depends on $\boldsymbol{\xi}_N$. Total Helmholtz free energy changes inside the volume are given as

$$\Delta\bar{W}_{\text{micro}} = \sum_{N=1}^{8}\Delta\bar{W}_N(\boldsymbol{\xi}_N). \tag{22}$$

4.3 Strain gradient elasticity continuum model

We substitute each $\boldsymbol{\xi}_N$ ($N = 1, 2, ..., 8$) into Eqs. (16) and (21), sum up and rearrange terms to form scalar invariants.[2] Eventually, we arrive at the following expression:

$$\Delta\bar{W}_{\text{micro}} = \frac{16}{3}E_{ii} + \frac{8}{3}E_{ij}E_{ij} + \frac{1}{3}H_{ijk}H_{ijk} - \frac{1}{6}H_{ijj}H_{ikk} =: \bar{W}_{\text{macro}}. \tag{23}$$

Restoring dimensions of all quantities using $H_{ijk} = LD_{ijk}$ and $W_{\text{macro}} := \frac{3}{2}k_{\text{B}}T\left(\bar{W}_{\text{macro}}\right)$, we obtain

$$W_{\text{macro}} = \frac{3}{2}k_{\text{B}}T\left(\frac{16}{3}E_{ii} + \frac{8}{3}E_{ij}E_{ij} + \frac{L^2}{3}D_{ijk}D_{ijk} - \frac{L^2}{6}D_{ijj}D_{ikk}\right). \tag{24}$$

With introducing density n of chains (number of chains per unit volume), the free energy density w can be expressed in terms of averages of strain $\langle\varepsilon_{ij}\rangle$ and strain gradient $\langle\varepsilon_{ijk}\rangle$ given in Eq. (14) as

$$w = \frac{W_{\text{macro}}}{8}n = nk_{\text{B}}T\left(\langle\varepsilon_{ii}\rangle + \frac{1}{2}\langle\varepsilon_{ij}\rangle\langle\varepsilon_{ij}\rangle + \frac{L^2}{16}\langle\varepsilon_{ij,k}\rangle\langle\varepsilon_{ij,k}\rangle - \frac{L^2}{32}\langle\varepsilon_{ij,j}\rangle\langle\varepsilon_{ik,k}\rangle\right). \tag{25}$$

We interpret independent variables in continuum models as the volume averages $\langle\varepsilon_{ij}\rangle$, $\langle\varepsilon_{ij,k}\rangle$, get rid of the square brackets, and arrive at the constitutive model in the form of free energy

$$w\left(\varepsilon_{ij}(\boldsymbol{x}), \varepsilon_{ij,k}(\boldsymbol{x})\right) = nk_{\text{B}}T\left(\varepsilon_{ii} + \frac{1}{2}\varepsilon_{ij}\varepsilon_{ij} + \frac{L^2}{16}\varepsilon_{ij,k}\varepsilon_{ij,k} - \frac{L^2}{32}\varepsilon_{ij,j}\varepsilon_{ik,k}\right), \tag{26}$$

where $\boldsymbol{x} \in V_{\text{continuum}}$ *denotes material points of the whole structure from now on*, and the strain energy renders a spatially varying function only through its dependence on strain $\varepsilon_{ij}(\boldsymbol{x})$ and strain gradient $\varepsilon_{ij,k}(\boldsymbol{x})$.

[2] This is a lengthy calculation, simplified by non-dimensionalization to some extent.

One of the most questions of common interest is whether the classical continuum theory can be recovered from the proposed strain gradient theory when considering a neglectable strain gradient effect. That is, when the intrinsic characteristic length L of strain gradient continuum is much smaller than geometric dimensions of the whole structure, the constitutive relation shall reduce to its classical counterpart. In case of the original work where the eight-chain model is proposed (refer to Eq. (21) in Arruda and Boyce [12]), the strain energy density w_c can actually be expressed as

$$w_c = nk_{\mathrm{B}}T\left(\frac{1}{2}\left(I_1 - 3\right) + \mathcal{O}\left(I_1^2\right)\right), \tag{27}$$

where the so-called first invariant has the relation: $I_1 = \lambda_1^2 + \lambda_2^2 + \lambda_3^2$, with $\lambda_1, \lambda_2, \lambda_3$ representing the stretch values of the representative volume along three directions. The truncation error of the strain energy density w_c is $\mathcal{O}\left(I_1^2\right)$.

For infinitesimal deformations, $\lambda_1 \to 1, \lambda_2 \to 1, \lambda_3 \to 1$, permitting the following representation:

$$\begin{aligned} \lambda_1 &= 1 + \varepsilon_{11}, \\ \lambda_2 &= 1 + \varepsilon_{22}, \\ \lambda_3 &= 1 + \varepsilon_{33} \end{aligned} \tag{28}$$

with $\varepsilon_{11} \to 0, \varepsilon_{22} \to 0, \varepsilon_{33} \to 0$. Substituting Eq. (28) into Eq. (27) and getting rid of higher-order terms, we get

$$\begin{aligned} w_c &= nk_{\mathrm{B}}T\left(\varepsilon_{11} + \varepsilon_{22} + \varepsilon_{33} + \frac{1}{2}\left(\varepsilon_{11}^2 + \varepsilon_{22}^2 + \varepsilon_{33}^2\right)\right) \\ &= nk_{\mathrm{B}}T\left(\varepsilon_{ii} + \frac{1}{2}\varepsilon_{ij}\varepsilon_{ij}\right). \end{aligned} \tag{29}$$

It is clear that the classical eight-chain model (29) can be recovered from the proposed strain gradient model (26) when neglecting the strain gradient effect ($L = 0$). It shall be noted that in addition to the classical eight-chain model (29), many other statistical mechanics models have been developed, including the 3-chain network model, the 4-chain network model, and the full network model [8]. It is hopeful that the proposed framework of strain gradient theory can also be used for developing their strain gradient counterparts based on a similar procedure in Sect. 3.2.

Furthermore, we have the following remarks for the constitutive relation defined by the proposed strain gradient model (26).

(a) The constitutive relation (26) describes a first-order strain gradient continuum, and more specifically, it belongs to the simplified strain gradient elasticity theory (SSGET [38,39]) according to the scalar invariants of strain gradient tensor in use, justifying the assumption on parameter reduction.
(b) The intrinsic characteristic length L now has a natural and unambiguous physical meaning, i.e., size (side length) of the representative network shown in Fig. 3.
(c) There exists a hydrostatic residual stress:

$$\sigma_{ij}^{(0)} = \left.\frac{\partial w}{\partial \varepsilon_{ij}}\right|_{\varepsilon_{ij}=0} = nk_B T\delta_{ij}, \tag{30}$$

where δ_{ij} is the Kronecker delta.
(d) Only two parameters ($nk_{\mathrm{B}}T$, L) need to be calibrated.

5 Application to static bending of beams

In this section, we aim at the illustration of how to apply the proposed strain gradient model (26) to different beam models, and correspondingly, the size-dependent behaviors can be examined.

Note that starting from Eq. (26), we use the notation $\boldsymbol{x} \in V_{\text{continuum}}$ to denote material points of the whole structure. In the following context, the zero hydrostatic residual stress in Eq. (30) is invoked, i.e., $\sigma_{ij}^{(0)} = 0$, and correspondingly the free energy density (26) can be simplified as

$$w\left(\varepsilon_{ij}\left(\boldsymbol{x}\right), \varepsilon_{ij,k}\left(\boldsymbol{x}\right)\right) = nk_{\mathrm{B}}T\left(\frac{1}{2}\varepsilon_{ij}\varepsilon_{ij} + \frac{L^2}{16}\varepsilon_{ij,k}\varepsilon_{ij,k} - \frac{L^2}{32}\varepsilon_{ij,j}\varepsilon_{ik,k}\right). \tag{31}$$

Consider a rectangular Euler–Bernoulli beam with thickness h and width b much smaller than its length l. The displacement field of Euler–Bernoulli beam theory can be given by

$$\begin{aligned} u_1 &= -x_3\frac{\mathrm{d}u_3}{\mathrm{d}x_1}, \\ u_2 &= 0, \\ u_3 &= u_3\left(x_1\right), \end{aligned} \tag{32}$$

where $0 \le x_1 \le l$, $-b/2 \le x_2 \le b/2$, $-h/2 \le x_3 \le h/2$. The only nonzero components of strain and strain gradient tensors are

$$\begin{aligned} \varepsilon_{11} &= -x_3\frac{\mathrm{d}^2u_3}{\mathrm{d}x_1^2}, \\ \varepsilon_{11,1} &= -x_3\frac{\mathrm{d}^3u_3}{\mathrm{d}x_1^3}, \\ \varepsilon_{11,3} &= -\frac{\mathrm{d}^2u_3}{\mathrm{d}x_1^2}. \end{aligned} \tag{33}$$

The stain gradient in the thickness direction is non-zero, although the strain component in the thickness direction is zero. The size-dependent effect of $\varepsilon_{11,3}$ is often assumed to be neglected in the size-dependent model of beams and plates, originally aiming at reducing the complexity of size-dependent beam and plate models [45]. It shall be noted that the effect of the stain gradient in the thickness direction plays a very important role in statics and dynamics of beams [45–47].

5.1 Size dependence in the viewpoint of free energy

Theories of strain gradient elasticity are often applied to explain the size-effects. Now we want to find out: *at what scale of the thickness h, will the variation of mechanical properties be observable?* In other words, the strain gradient-induced elastic energy is non-negligible compared to the strain energy. Integrating the energy density (31) along the thickness using (33), taking the ratio γ of strain gradient-induced energy to strain-induced energy, we get

$$\gamma := \frac{L^2\left(\frac{\mathrm{d}^3u_3}{\mathrm{d}x_1^3}\right)^2\frac{h^3}{12} + 2L^2\left(\frac{\mathrm{d}^2u_3}{\mathrm{d}x_1^2}\right)^2 h}{16\left(\frac{\mathrm{d}^2u_3}{\mathrm{d}x_1^2}\right)^2\frac{h^3}{12}} = \frac{1}{16}\left(\frac{L}{\ell^{\mathrm{def}}}\right)^2 + \frac{3}{2}\left(\frac{L}{h}\right)^2, \tag{34}$$

where we define the characteristic length of deformation ℓ^{def} as follows:

$$\begin{aligned} \ell^{\mathrm{def}} &= \phi/\phi', \\ \phi &:= \frac{\mathrm{d}^2u_3}{\mathrm{d}x_1^2}, \\ \phi' &:= \frac{\mathrm{d}\phi}{\mathrm{d}x_1} = \frac{\mathrm{d}^3u_3}{\mathrm{d}x_1^3}. \end{aligned} \tag{35}$$

Here we have three length scales:

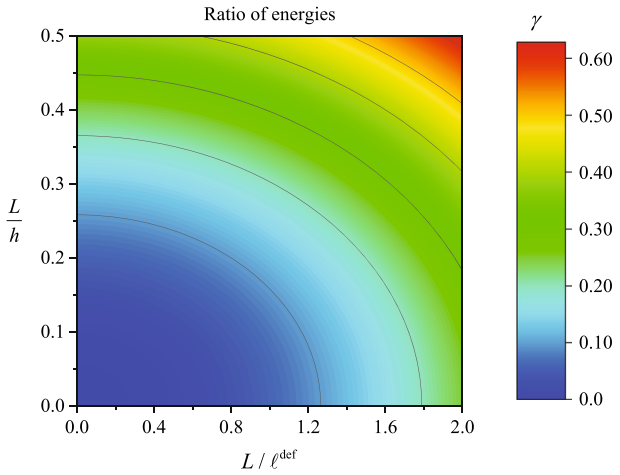

Fig. 4 Size-dependent ratio of energies

(a) characteristic length L of the strain gradient material,
(b) beam thickness h,
(c) deformation characteristic length ℓ^{def}.

When either h or ℓ^{def} is closed to L, the strain gradient-induced energy will account for a large portion of the total free energy, thus exhibiting significant size effects. A quantitative study is shown in Fig. 4.

5.2 Governing equation in terms of displacement field and effective bending rigidity

In the following, we shall take a closer look at the effective mechanical properties affected by the beam thickness h. To examine the size dependence of mechanical properties, we derive the equations of motion using the principle of virtual work.

To simplify derivations, the strain energy density (31) can be, alternatively, expressed as

$$w = \mu\varepsilon_{ij}\varepsilon_{ij} + A_1\varepsilon_{ij,k}\varepsilon_{ij,k} + A_2\varepsilon_{ij,j}\varepsilon_{ik,k}, \tag{36}$$

where we have defined

$$\begin{aligned} \mu &:= \frac{1}{2}nk_{\mathrm{B}}T, \\ A_1 &:= \frac{L^2}{16}nk_{\mathrm{B}}T, \\ A_2 &:= -\frac{L^2}{32}nk_{\mathrm{B}}T. \end{aligned} \tag{37}$$

In what follows, the proposed strain gradient model (36) is used to predict different results for static bending of two different beam models in the framework of Euler–Bernoulli beam theory: one-dimensional beam model and three-dimensional beam model.

5.2.1 One-dimensional beam model

This subsection is based on the assumption that the strain gradient Euler–Bernoulli beam can be physically viewed as an one-dimensional model, where the effect of boundary conditions on the top and bottom surfaces of the beam is assumed to be neglectable [48].

Plugging in the strain field (33), the constitute relation (36) can be expanded as

$$w = \mu(x_3)^2\left(\frac{\mathrm{d}^2u_3}{\mathrm{d}x_1^2}\right)^2 + (A_1 + A_2)\,(x_3)^2\left(\frac{\mathrm{d}^3u_3}{\mathrm{d}x_1^3}\right)^2 + A_1\left(\frac{\mathrm{d}^2u_3}{\mathrm{d}x_1^2}\right)^2. \tag{38}$$

The total strain energy is given as the integral over the entire beam volume V

$$W = \int_V w \mathrm{d}V \tag{39}$$

which can be expressed as

$$W = \mu I \int_0^l \left(\frac{\mathrm{d}^2 u_3}{\mathrm{d}x_1^2}\right)^2 \mathrm{d}x_1 + (A_1 + A_2)\, I \int_0^l \left(\frac{\mathrm{d}^3 u_3}{\mathrm{d}x_1^3}\right)^2 \mathrm{d}x_1 + A_1 a \int_0^l \left(\frac{\mathrm{d}^2 u_3}{\mathrm{d}x_1^2}\right)^2 \mathrm{d}x_1 \tag{40}$$

with the definitions

$$\begin{aligned} I &:= b \int_{-h/2}^{h/2} (x_3)^2 \mathrm{d}x_3, \\ a &:= b \int_{-h/2}^{h/2} \mathrm{d}x_3. \end{aligned} \tag{41}$$

Next, we invoke the principle of virtual work to derive the governing equations and boundary conditions. The first variation of the total strain energy is

$$\delta W = \mu I \delta \left[\int_0^l \left(\frac{\mathrm{d}^2 u_3}{\mathrm{d}x_1^2}\right)^2 \mathrm{d}x_1\right] + (A_1 + A_2)\, I \delta \left[\int_0^l \left(\frac{\mathrm{d}^3 u_3}{\mathrm{d}x_1^3}\right)^2 \mathrm{d}x_1\right] + A_1 a \delta \left[\int_0^l \left(\frac{\mathrm{d}^2 u_3}{\mathrm{d}x_1^2}\right)^2 \mathrm{d}x_1\right], \tag{42}$$

where δ denotes the variational operator. Integrating by parts, we obtain

$$\begin{aligned} \delta W = & \int_0^l \left(2\,(\mu I + A_1 a)\left(\frac{\mathrm{d}^4 u_3}{\mathrm{d}x_1^4}\right) - 2\,(A_1 + A_2)\, I \left(\frac{\mathrm{d}^6 u_3}{\mathrm{d}x_1^6}\right)\right) \delta u_3 \mathrm{d}x_1 \\ & + \mu I \left(\left[2\left(\frac{\mathrm{d}^2 u_3}{\mathrm{d}x_1^2}\right)\delta\left(\frac{\mathrm{d}u_3}{\mathrm{d}x_1}\right)\right]_0^l - \left[2\left(\frac{\mathrm{d}^3 u_3}{\mathrm{d}x_1^3}\right)\delta u_3\right]_0^l\right) \\ & + (A_1 + A_2)\, I \left(\left[2\left(\frac{\mathrm{d}^3 u_3}{\mathrm{d}x_1^3}\right)\delta\left(\frac{\mathrm{d}^2 u_3}{\mathrm{d}x_1^2}\right)\right]_0^l - \left[2\left(\frac{\mathrm{d}^4 u_3}{\mathrm{d}x^4}\right)\delta\left(\frac{\mathrm{d}u_3}{\mathrm{d}x}\right)\right]_0^l + \left[2\left(\frac{\mathrm{d}^5 u_3}{\mathrm{d}x^5}\right)\delta u_3\right]_0^l\right) \\ & + A_1 a \left(\left[2\left(\frac{\mathrm{d}^2 u_3}{\mathrm{d}x_1^2}\right)\delta\left(\frac{\mathrm{d}u_3}{\mathrm{d}x_1}\right)\right]_0^l - \left[2\left(\frac{\mathrm{d}^3 u_3}{\mathrm{d}x_1^3}\right)\delta u_3\right]_0^l\right). \end{aligned} \tag{43}$$

The external load potential is assumed as

$$P = -\left[Q u_3 + M\left(\frac{\mathrm{d}u_3}{\mathrm{d}x_1}\right) + M_h\left(\frac{\mathrm{d}^2 u_3}{\mathrm{d}x_1^2}\right)\right]_0^l - \int_0^l q u_3 \mathrm{d}x_1, \tag{44}$$

where q is the distributed load, and the rest are applied at the beam ends: Q is the external shear force, M is the external moment, and M_h is the external higher-order moment. The first variation of the external load potential is given as

$$\delta P = -\left[Q\delta u_3 + M\delta\left(\frac{\mathrm{d}u_3}{\mathrm{d}x_1}\right) + M_h\delta\left(\frac{\mathrm{d}^2 u_3}{\mathrm{d}x_1^2}\right)\right]_0^l - \int_0^l q\delta u_3 \mathrm{d}x_1. \tag{45}$$

Invoking the principle of virtual work, i.e.,

$$\delta W + \delta P = 0, \tag{46}$$

we get

$$\begin{aligned}\delta W+\delta P=&\int_0^l\left(2\left(\mu I+A_1a\right)\left(\frac{\mathrm{d}^4u_3}{\mathrm{d}x_1^4}\right)-2\left(A_1+A_2\right)I\left(\frac{\mathrm{d}^6u_3}{\mathrm{d}x_1^6}\right)-q\right)\delta u_3\mathrm{d}x_1\\&+\left[\left(-2\left(\mu I+A_1a\right)\left(\frac{\mathrm{d}^3u_3}{\mathrm{d}x_1^3}\right)+2\left(A_1+A_2\right)I\left(\frac{\mathrm{d}^5u_3}{\mathrm{d}x^5}\right)-Q\right)\delta u_3\right]_0^l\\&+\left[\left(2\left(\mu I+A_1a\right)\left(\frac{\mathrm{d}^2u_3}{\mathrm{d}x_1^2}\right)-2\left(A_1+A_2\right)I\left(\frac{\mathrm{d}^4u_3}{\mathrm{d}x^4}\right)-M\right)\delta\left(\frac{\mathrm{d}u_3}{\mathrm{d}x_1}\right)\right]_0^l\\&+\left[\left(2\left(A_1+A_2\right)I\left(\frac{\mathrm{d}^3u_3}{\mathrm{d}x_1^3}\right)-M_h\right)\delta\left(\frac{\mathrm{d}^2u_3}{\mathrm{d}x_1^2}\right)\right]_0^l.\end{aligned}\tag{47}$$

Thus, we obtain the size-dependent equation of motion

$$2\left(\mu I+A_1a\right)\left(\frac{\mathrm{d}^4u_3}{\mathrm{d}x_1^4}\right)-2\left(A_1+A_2\right)I\left(\frac{\mathrm{d}^6u_3}{\mathrm{d}x_1^6}\right)-q=0,$$

and the boundary conditions

$$\begin{aligned}-2\left(\mu I+A_1a\right)\left(\frac{\mathrm{d}^3u_3}{\mathrm{d}x_1^3}\right)+2\left(A_1+A_2\right)I\left(\frac{\mathrm{d}^5u_3}{\mathrm{d}x^5}\right)-Q=0,\\2\left(\mu I+A_1a\right)\left(\frac{\mathrm{d}^2u_3}{\mathrm{d}x_1^2}\right)-2\left(A_1+A_2\right)I\left(\frac{\mathrm{d}^4u_3}{\mathrm{d}x^4}\right)-M=0,\\2\left(A_1+A_2\right)I\left(\frac{\mathrm{d}^3u_3}{\mathrm{d}x_1^3}\right)-M_h=0.\end{aligned}$$

For the sake of simplification, as usual, we focus on the cases where the beam's neutral axis has a constant curvature [30,49–51], that is,

$$\frac{\mathrm{d}^2u_3}{\mathrm{d}x_1^2}=\text{constant}.\tag{48}$$

When considering a cantilevered beam subject to an external moment M at its end ($x_1=l$), from Eqs. (47) and (48), we arrive at the following relation for the proposed strain gradient theory:

$$2\left(\mu I+A_1a\right)\left(\frac{\mathrm{d}^2u_3}{\mathrm{d}x_1^2}\right)=M.\tag{49}$$

If the effect of strain gradient is neglectable ($A_1=0$), the previous equation can be simplified to that of classical continuum theory of elasticity:

$$2\mu I\frac{\mathrm{d}^2u_3}{\mathrm{d}x_1^2}=M.\tag{50}$$

The classical bending rigidity can be easily identified as $2\mu I$. As we know, the classical bending rigidity for a cantilevered beam is EI where E denotes Young's modulus. Thus, Young's modulus E can be viewed as 2μ, that is,

$$E=2\mu.\tag{51}$$

Note that, for the isotropic material, Young's modulus E have the following relation:

$$E=\frac{\mu\left(3\lambda+2\mu\right)}{\lambda+\mu},\tag{52}$$

where λ and μ are the Lamé constants. As mentioned before, since the material property of the 8-chain network model is characterized by one modulus, we have the relation $\lambda = 0$. Thus, the classical isotropic relation (52) can be simplified to Eq. (51).

Clearly, with the help of the definition (37), the microscopic physical meaning for Young's modulus E in the viewpoint of statistical mechanics can be given by

$$E = nk_{\mathrm{B}}T.$$

5.2.2 Size dependence of one-dimensionally physical model

To explore the size dependence of the proposed strain gradient theory of elasticity, the effective bending rigidity of Eq. (49) can be obtained in a familiar way [49] as

$$R_{\mathrm{eff}} := \frac{M}{\left(\frac{\mathrm{d}^2 u_3}{\mathrm{d}x_1^2}\right)} = EI + 2A_1 a. \tag{53}$$

The first term actually stands for the classical counterpart (classical bending rigidity R_{cl}). To see this, we note from expression of the strain energy density (36) that the stress tensor is

$$\sigma_{ij} := \frac{\partial w}{\partial \varepsilon_{ij}} = 2\mu\varepsilon_{ij} = E\varepsilon_{ij}, \tag{54}$$

and ultimately we can arrive at the result

$$EI = \frac{\int_S \sigma_{11}\,(-x_3)\,\mathrm{d}S}{\frac{\mathrm{d}^2 u_3}{\mathrm{d}x_1^2}} =: R_{\mathrm{cl}}, \tag{55}$$

which is the well-known classical bending rigidity and justify the discussion below Eq. (50) . With the help of the expression (55) of classical bending rigidity, Eq. (53) can be alternatively expressed as

$$R_{\mathrm{eff}} = R_{\mathrm{cl}} + 2A_1 a. \tag{56}$$

The normalized effective bending rigidity is

$$\bar{R}_{\mathrm{eff}} := \frac{R_{\mathrm{eff}}}{R_{\mathrm{cl}}} = 1 + \frac{L^2}{8}\frac{a}{I}, \tag{57}$$

where Eq. (37) is used. Recall that the area of cross-section a and the moment of inertia I have been defined in Eq. (41), and L is the intrinsic length scale of strain gradient material. Plugging in the beam's width b and height h, $\bar{R}_{\mathrm{eff}}$ renders

$$\frac{R_{\mathrm{eff}}}{R_{\mathrm{cl}}} = 1 + \frac{3}{2}\left(\frac{L}{h}\right)^2, \tag{58}$$

which in turn implies that there will be significant variations in normalized bending rigidity when the characteristic length L of the strain gradient material cannot be neglected compared to the beam thickness h. In addition, Eq. (58) presents a typical type of size-dependence shown by existing literature. For example, in Niiranen et al. [52], it is shown how several generalized beam models share the same tendency as Eq. (58), and in Korshunova et al. [53], the origin of such tendency is clarified in the context of 3D octet-truss lattice beams.

5.2.3 Three-dimensionally physical beam model

In this subsection, the strain gradient Euler–Bernoulli beam is thought of as a three-dimensionally physical model, and therefore the boundary conditions on the top and bottom surfaces of the beam are considered [54–56].

From the strain energy density (36), the stress tensor and the hyper-stress tensor can be obtained as

$$\begin{aligned} \sigma_{ij} &:= \frac{\partial w}{\partial \varepsilon_{ij}} = 2\mu\varepsilon_{ij}, \\ \tau_{ijk} &:= \frac{\partial w}{\partial \varepsilon_{ij,k}} = 2A_1\varepsilon_{ij,k} + 2A_2\delta_{jk}\varepsilon_{im,m}. \end{aligned} \tag{59}$$

Using the strain tensor components (33), we obtain all the non-zero components from the previous equations as

$$\begin{aligned} \sigma_{11} &= 2\mu\varepsilon_{11} = 2\mu\left(-x_3\frac{\mathrm{d}^2u_3}{\mathrm{d}x_1^2}\right), \\ \tau_{111} &= 2\left(A_1+A_2\right)\varepsilon_{11,1} = 2\left(A_1+A_2\right)\left(-x_3\frac{\mathrm{d}^3u_3}{\mathrm{d}x_1^3}\right), \\ \tau_{113} &= 2A_1\varepsilon_{11,3} = 2A_1\left(-\frac{\mathrm{d}^2u_3}{\mathrm{d}x_1^2}\right). \end{aligned} \tag{60}$$

The variation of strain energy can then be given as

$$\delta W = b\int_0^l\int_{-h/2}^{h/2}\left(\sigma_{11}\delta\varepsilon_{11} + \tau_{111}\delta\varepsilon_{11,1} + \tau_{113}\delta\varepsilon_{11,3}\right)\mathrm{d}x_3\mathrm{d}x_1. \tag{61}$$

Using the displacement field defined in Eq. (32), the previous expression becomes

$$\delta W = b\int_0^l\int_{-h/2}^{h/2}\left(\sigma_{11}\delta u_{1,1} + \tau_{111}\delta u_{1,11} + \tau_{113}\delta u_{1,13}\right)\mathrm{d}x_3\mathrm{d}x_1. \tag{62}$$

Integrating by parts with respect variable x_3, we get

$$\delta W = b\int_0^l\int_{-h}^{h}\left(\sigma_{11}\delta u_{1,1} + \tau_{111}\delta u_{1,11} - \tau_{113,3}\delta u_{1,1}\right)\mathrm{d}x_3\mathrm{d}x_1 + b\int_0^l\left[\tau_{113}\delta u_{1,1}\right]_{-h/2}^{h/2}\mathrm{d}x_1. \tag{63}$$

Integrating by parts again with respect variable x_1, we get

$$\begin{aligned} \delta W = {} & b\int_{-h/2}^{h/2}\int_0^l\left(-\sigma_{11,1} + \tau_{111,11} + \tau_{113,31}\right)\delta u_1\mathrm{d}x_1\mathrm{d}x_3 \\ & + b\int_{-h/2}^{h/2}\left[\left(\sigma_{11} - \tau_{111,1} - \tau_{113,3}\right)\delta u_1 + \tau_{111}\delta u_{1,1}\right]_{x_1=0}^{x_1=l}\mathrm{d}x_3 \\ & - b\int_0^l\left[\tau_{113,1}\delta u_1\right]_{z=-h/2}^{z=h/2}\mathrm{d}x_1 + b\left[\left[\tau_{113}\delta u_1\right]_{x_1=0}^{x_1=l}\right]_{z=-h/2}^{z=h/2}. \end{aligned} \tag{64}$$

From the last two terms, we get the surface conditions

$$\tau_{113,1} = 0 \text{ on } z = \pm h/2 \tag{65}$$

and the edge conditions

$$\tau_{113} = 0 \text{ on } z = \pm h \cap x = 0, l. \tag{66}$$

Substituting back to Eq. (64) and noting that $\tau_{113,3} = 0$, the variation of strain energy reduces to

$$\begin{aligned}\delta W = b\int_{-h/2}^{h/2}\int_0^l \left(-\sigma_{11,1} + \tau_{111,11}\right)\delta u_1 \mathrm{d}x_1\mathrm{d}x_3 \\ + b\int_{-h/2}^{h/2}\left[\left(\sigma_{11} - \tau_{111,1}\right)\delta u_1 + \tau_{111}\delta u_{1,1}\right]_{x_1=0}^{x_1=l}\mathrm{d}x_3.\end{aligned} \tag{67}$$

Using the expressions of the stress and hyper-stress (60) and the following relations

$$\begin{aligned}\delta u_1 &= -x_3\frac{\mathrm{d}\delta u_3}{\mathrm{d}x_1}, \\ \delta u_{1,1} &= -x_3\frac{\mathrm{d}^2\delta u_3}{\mathrm{d}^2x_1},\end{aligned} \tag{68}$$

we get

$$\begin{aligned}\delta W = \int_0^l \left(2\mu I\left(\frac{\mathrm{d}^4u_3}{\mathrm{d}x_1^4}\right) - 2\left(A_1+A_2\right)I\left(\frac{\mathrm{d}^6u_3}{\mathrm{d}x_1^6}\right)\right)\delta u_3\mathrm{d}x_1 \\ + \left[\left(-2\mu I\left(\frac{\mathrm{d}^3u_3}{\mathrm{d}x_1^3}\right) + 2\left(A_1+A_2\right)I\left(\frac{\mathrm{d}^5u_3}{\mathrm{d}x_1^5}\right)\right)\delta u_3\right]_0^l \\ + \left[\left(2\mu I\left(\frac{\mathrm{d}^2u_3}{\mathrm{d}x_1^2}\right) - 2\left(A_1+A_2\right)I\left(\frac{\mathrm{d}^4u_3}{\mathrm{d}x_1^4}\right)\right)\delta\left(\frac{\mathrm{d}u_3}{\mathrm{d}x_1}\right)\right]_0^l \\ + \left[\left(2\left(A_1+A_2\right)I\left(\frac{\mathrm{d}^3u_3}{\mathrm{d}x_1^3}\right)\right)\delta\left(\frac{\mathrm{d}^2u_3}{\mathrm{d}^2x_1}\right)\right]_0^l.\end{aligned} \tag{69}$$

Variation of the external load potential is already given in Eq. (45), for the sake of readability, we write it herein as

$$\delta P = -\left[Q\delta u_3 + M\delta\left(\frac{\mathrm{d}u_3}{\mathrm{d}x_1}\right) + M_h\delta\left(\frac{\mathrm{d}^2u_3}{\mathrm{d}x_1^2}\right)\right]_0^l - \int_0^l q\delta u_3\mathrm{d}x_1,$$

which gives the total variation as

$$\begin{aligned}\delta W + \delta P = \int_0^l \left(2\mu I\left(\frac{\mathrm{d}^4u_3}{\mathrm{d}x_1^4}\right) - 2\left(A_1+A_2\right)I\left(\frac{\mathrm{d}^6u_3}{\mathrm{d}x_1^6}\right) - q\right)\mathrm{d}x_1 \\ + \left[\left(-2\mu I\left(\frac{\mathrm{d}^3u_3}{\mathrm{d}x_1^3}\right) + 2\left(A_1+A_2\right)I\left(\frac{\mathrm{d}^5u_3}{\mathrm{d}x_1^5}\right) - Q\right)\delta u_3\right]_0^l \\ + \left[\left(2\mu I\left(\frac{\mathrm{d}^2u_3}{\mathrm{d}x_1^2}\right) - 2\left(A_1+A_2\right)I\left(\frac{\mathrm{d}^4u_3}{\mathrm{d}x_1^4}\right) - M\right)\delta\left(\frac{\mathrm{d}u_3}{\mathrm{d}x_1}\right)\right]_0^l \\ \left[\left(2\left(A_1+A_2\right)I\left(\frac{\mathrm{d}^3u_3}{\mathrm{d}x_1^3}\right) - M_h\right)\delta\left(\frac{\mathrm{d}^2u_3}{\mathrm{d}^2x_1}\right)\right]_0^l.\end{aligned} \tag{70}$$

Invoking the principle of virtual work, we get the governing equation

$$2\mu I\left(\frac{\mathrm{d}^4u_3}{\mathrm{d}x_1^4}\right) - 2\left(A_1+A_2\right)I\left(\frac{\mathrm{d}^6u_3}{\mathrm{d}x_1^6}\right) - q = 0$$

and the boundary conditions

$$-2\mu I\left(\frac{\mathrm{d}^3u_3}{\mathrm{d}x_1^3}\right)+2\left(A_1+A_2\right)I\left(\frac{\mathrm{d}^5u_3}{\mathrm{d}x_1^5}\right)-Q=0,$$
$$2\mu I\left(\frac{\mathrm{d}^2u_3}{\mathrm{d}x_1^2}\right)-2\left(A_1+A_2\right)I\left(\frac{\mathrm{d}^4u_3}{\mathrm{d}x_1^4}\right)-M=0,$$
$$2\left(A_1+A_2\right)I\left(\frac{\mathrm{d}^3u_3}{\mathrm{d}x_1^3}\right)-M_h=0.$$

To compare with the one-dimensional beam model, considering also a cantilevered beam subject to an external moment M at its end ($x_1 = l$) and applying the assumption of constant curvature (48), we arrive at the following relation:

$$2\mu I\left(\frac{\mathrm{d}^2u_3}{\mathrm{d}x_1^2}\right)=M,$$

which is the same as the classical relation (50). Thus for static bending, the three-dimensional beam model results in a size-independent model as

$$R_{\mathrm{eff}}=R_{\mathrm{cl}}.$$

Here we provide the counterparts (Eqs. (49) and (58)) in the one-dimensional beam model for convenient comparison:

$$2\mu\left(I+A_1a\right)\left(\frac{\mathrm{d}^2u_3}{\mathrm{d}x_1^2}\right)=M,$$
$$\frac{R_{eff}}{R_{cl}}=1+\frac{3}{2}\left(\frac{L}{h}\right)^2.$$

6 Conclusions

In the present work, a general framework is proposed where the connection between chain conformations and strain gradient continuum configurations is established. The continuum displacement field is taken to be interpolatory at the chain ends. The framework enables to construct statistically based (physically based) strain gradient continuum constitutive relations. Applying the general framework, which puts no restriction on the geometry of the network, to a 8-chain network, we derive a first-order strain gradient material. There are two important results. First, the size of the representative network turns out to be the characteristic length scale of the strain gradient material. Second, only two scalar invariants of the strain gradient tensor remain at last, thus justifying the assumption on parameter reduction made in the simplified strain gradient elasticity theory. With the help of the proposed physically based strain gradient continuum theory, the microscopic physical meaning of elastic modulus and high-order elastic constant is clear.

Acknowledgements This work is supported by the National Natural Science Foundation of China (Grant No. 52175095) and the Young Top-notch Talent Cultivation Program of Hubei Province, China.

References

1. Marckmann, G., Verron, E.: Comparison of hyperelastic models for rubber-like materials. Rubber Chem. Technol. **79**(5), 835–858 (2006)
2. Manias, E., Chen, J., Fang, N., Zhang, X.: Polymeric micromechanical components with tunable stiffness. Appl. Phys. Lett. **79**(11), 1700–1702 (2001)
3. Lam, D.C., Yang, F., Chong, A., Wang, J., Tong, P.: Experiments and theory in strain gradient elasticity. J. Mech. Phys. Solids **51**(8), 1477–1508 (2003)

4. Rubinstein, M., Colby, R.H., et al.: Polymer physics, vol. 23. Oxford University Press, New York (2003)
5. Treloar, L.G.: The physics of rubber elasticity
6. Treloar, L.: Stress-strain data for vulcanized rubber under various types of deformation. Rubber Chem. Technol. **17**(4), 813–825 (1944)
7. Wall, F.T.: Statistical thermodynamics of rubber. II. J. Chem. Phys. **10**(7), 485–488 (1942)
8. Boyce, M.C., Arruda, E.M.: Constitutive models of rubber elasticity: a review. Rubber Chem. Technol. **73**(3), 504–523 (2000)
9. Wang, M.C., Guth, E.: Statistical theory of networks of non-Gaussian flexible chains. J. Chem. Phys. **20**(7), 1144–1157 (1952)
10. Treloar, L.: The elasticity of a network of long-chain molecules-III. Trans. Faraday Soc. **42**, 83–94 (1946)
11. Flory, P.J., Rehner, J., Jr.: Statistical mechanics of cross-linked polymer networks I rubberlike elasticity. J. Chem. Phys. **11**(11), 512–520 (1943)
12. Arruda, E.M., Boyce, M.C.: A three-dimensional constitutive model for the large stretch behavior of rubber elastic materials. J. Mech. Phys. Solids **41**(2), 389–412 (1993)
13. Miehe, C., Göktepe, S., Lulei, F.: A micro-macro approach to rubber-like materials-part I: the non-affine micro-sphere model of rubber elasticity. J. Mech. Phys. Solids **52**(11), 2617–2660 (2004)
14. Miehe, C., Göktepe, S.: A micro–macro approach to rubber-like materials. part II: The micro-sphere model of finite rubber viscoelasticity. J. Mech. Phys. Solids **53**(10), 2231–2258 (2005)
15. Göktepe, S., Miehe, C.: A micro-macro approach to rubber-like materials. Part III: The micro-sphere model of anisotropic Mullins-type damage. J. Mech. Phys. Solids **53**(10), 2259–2283 (2005)
16. Mindlin, R.D.: Second gradient of strain and surface-tension in linear elasticity. Int. J. Solids Struct. **1**(4), 417–438 (1965)
17. Mindlin, R.D., Eshel, N.: On first strain-gradient theories in linear elasticity. Int. J. Solids Struct. **4**(1), 109–124 (1968)
18. Yang, F., Chong, A., Lam, D.C.C., Tong, P.: Couple stress based strain gradient theory for elasticity. Int. J. Solids Struct. **39**(10), 2731–2743 (2002)
19. Eringen, A.C., Edelen, D.: On nonlocal elasticity. Int. J. Eng. Sci. **10**(3), 233–248 (1972)
20. Eringen, A.C.: Nonlocal Continuum Field Theories. Springer, New York (2002)
21. Eringen, A.C.: Microcontinuum Field Theories: I. Foundations and Solids. Springer, New York (2012)
22. Germain, P.: The method of virtual power in continuum mechanics. Part 2: Microstructure. SIAM J. Appl. Math. **25**(3), 556–575 (1973)
23. Srinivasa, A.R., Reddy, J.: An overview of theories of continuum mechanics with nonlocal elastic response and a general framework for conservative and dissipative systems. Appl. Mech. Rev. **69**(3)
24. Rafii-Tabar, H., Ghavanloo, E., Fazelzadeh, S.A.: Nonlocal continuum-based modeling of mechanical characteristics of nanoscopic structures. Phys. Rep. **638**, 1–97 (2016)
25. Reddy, J.: Nonlocal theories for bending, buckling and vibration of beams. Int. J. Eng. Sci. **45**(2–8), 288–307 (2007)
26. Reddy, J.: Nonlocal nonlinear formulations for bending of classical and shear deformation theories of beams and plates. Int. J. Eng. Sci. **48**(11), 1507–1518 (2010)
27. Ghosh, S., Kumar, A., Sundararaghavan, V., Waas, A.M.: Non-local modeling of epoxy using an atomistically-informed kernel. Int. J. Solids Struct. **50**(19), 2837–2845 (2013)
28. Khodabakhshi, P., Reddy, J.: A unified integro-differential nonlocal model. Int. J. Eng. Sci. **95**, 60–75 (2015)
29. Lim, C., Zhang, G., Reddy, J.: A higher-order nonlocal elasticity and strain gradient theory and its applications in wave propagation. J. Mech. Phys. Solids **78**, 298–313 (2015)
30. Zhou, S., Li, A., Wang, B.: A reformulation of constitutive relations in the strain gradient elasticity theory for isotropic materials. Int. J. Solids Struct. **80**, 28–37 (2016)
31. Forest, S.: Homogenization methods and mechanics of generalized continua-part 2. Theor. Appl. Mech. **28–29**, 113–144 (2002)
32. Bacca, M., Bigoni, D., Dal Corso, F., Veber, D.: Mindlin second-gradient elastic properties from dilute two-phase Cauchy-elastic composites. Part I: Closed form expression for the effective higher-order constitutive tensor. Int. J. Solids Struct. **50**(24), 4010–4019 (2013)
33. Bacca, M., Bigoni, D., Dal Corso, F., Veber, D.: Mindlin second-gradient elastic properties from dilute two-phase Cauchy-elastic composites part II: Higher-order constitutive properties and application cases. Int. J. Solids Struct. **50**(24), 4020–4029 (2013)
34. Hütter, G.: Homogenization of a Cauchy continuum towards a micromorphic continuum. J. Mech. Phys. Solids **99**, 394–408 (2017)
35. Alavi, S., Ganghoffer, J., Reda, H., Sadighi, M.: Construction of micromorphic continua by homogenization based on variational principles. J. Mech. Phys. Solids **153**, 104278 (2021)
36. Admal, N.C., Marian, J., Po, G.: The atomistic representation of first strain-gradient elastic tensors. J. Mech. Phys. Solids **99**, 93–115 (2017)
37. Maranganti, R., Sharma, P.: A novel atomistic approach to determine strain-gradient elasticity constants: Tabulation and comparison for various metals, semiconductors, silica, polymers and the (ir) relevance for nanotechnologies. J. Mech. Phys. Solids **55**(9), 1823–1852 (2007)
38. Altan, B., Aifantis, E.: On some aspects in the special theory of gradient elasticity. J. Mech. Behav. Mater. **8**(3), 231–282 (1997)
39. Gao, X.-L., Park, S.: Variational formulation of a simplified strain gradient elasticity theory and its application to a pressurized thick-walled cylinder problem. Int. J. Solids Struct. **44**(22–23), 7486–7499 (2007)
40. Gitman, I.M., Askes, H., Aifantis, E.C.: The representative volume size in static and dynamic micro-macro transitions. Int. J. Fract. **135**(1), L3–L9 (2005)
41. Khakalo, S., Balobanov, V., Niiranen, J.: Modelling size-dependent bending, buckling and vibrations of 2D triangular lattices by strain gradient elasticity models: applications to sandwich beams and auxetics. Int. J. Eng. Sci. **127**, 33–52 (2018)

42. Khakalo, S., Niiranen, J.: Form II of Mindlin's second strain gradient theory of elasticity with a simplification: for materials and structures from nano-to macro-scales. European Journal of Mechanics-A/Solids **71**, 292–319 (2018)
43. Solyaev, Y.: Self-consistent assessments for the effective properties of two-phase composites within strain gradient elasticity. Mech. Mater. 104321 (2022)
44. Gurtin, M.E., Fried, E., Anand, L.: The Mechanics and Thermodynamics of Continua. Cambridge University Press, Cambridge (2010)
45. Li, L., Tang, H., Hu, Y.: The effect of thickness on the mechanics of nanobeams. Int. J. Eng. Sci. **123**, 81–91 (2018)
46. Tang, H., Li, L., Hu, Y.: Coupling effect of thickness and shear deformation on size-dependent bending of micro/nano-scale porous beams. Appl. Math. Model. **66**, 527–547 (2019)
47. Tang, H., Li, L., Hu, Y., Meng, W., Duan, K.: Vibration of nonlocal strain gradient beams incorporating Poisson's ratio and thickness effects. Thin-Walled Struct. **137**, 377–391 (2019)
48. Lazopoulos, K., Lazopoulos, A.: Bending and buckling of thin strain gradient elastic beams. Eur. J. Mech.-A/Solids **29**(5), 837–843 (2010)
49. Li, L., Lin, R., Hu, Y.: Cross-section effect on mechanics of nonlocal beams. Arch. Appl. Mech. **91**(4), 1541–1556 (2021)
50. Li, L., Lin, R., Ng, T.Y.: Contribution of nonlocality to surface elasticity. Int. J. Eng. Sci. **152**, 103311 (2020)
51. Lin, Z., Wei, Y.: A strain gradient linear viscoelasticity theory. Int. J. Solids Struct. **203**, 197–209 (2020)
52. Niiranen, J., Balobanov, V., Kiendl, J., Hosseini, S.: Variational formulations, model comparisons and numerical methods for Euler-Bernoulli micro-and nano-beam models. Math. Mech. Solids **24**(1), 312–335 (2019)
53. Korshunova, N., Alaimo, G., Hosseini, S., Carraturo, M., Reali, A., Niiranen, J., Auricchio, F., Rank, E., Kollmannsberger, S.: Bending behavior of octet-truss lattice structures: modelling options, numerical characterization and experimental validation. Mater. Design **205**, 109693 (2021)
54. Papargyri-Beskou, S., Tsepoura, K., Polyzos, D., Beskos, D.: Bending and stability analysis of gradient elastic beams. Int. J. Solids Struct. **40**(2), 385–400 (2003)
55. Lurie, S., Solyaev, Y.: Revisiting bending theories of elastic gradient beams. Int. J. Eng. Sci. **126**, 1–21 (2018)
56. Lurie, S., Solyaev, Y.: On the formulation of elastic and electroelastic gradient beam theories. Continuum Mech. Thermodyn. **31**(6), 1601–1613 (2019)